Charged dopants in semiconductor nanowires under partially periodic boundary conditions

Tzu-Liang Chan, S. B. Zhang, and James R. Chelikowsky

Phys. Rev. B **83**, 245440 — Published 28 June 2011

DOI: 10.1103/PhysRevB.83.245440

Charged dopants in semiconductor nanowire under partially periodic boundary conditions

Tzu-Liang Chan[1,2], S. B. Zhang[2] and James R. Chelikowsky[1,3]
[1] *Center for Computational Materials, Institute for Computational Engineering and Sciences, University of Texas, Austin, Texas 78712, USA*
[2] *Department of Physics, Applied Physics, and Astronomy, Rensselaer Polytechnic Institute, Troy, New York 12180, USA*
[3] *Departments of Physics and Chemical Engineering, University of Texas, Austin, Texas 78712, USA*

We develop a one-dimensional, periodic real-space formalism for examining the electronic structure of charged nanowires from first-principles. The formalism removes spurious electrostatic interactions between charged unit cells by appropriately specifying a boundary condition for the Kohn-Sham equation. The resultant total energy of the charged system remains finite, and a Madelung-type correction is unnecessary. We demonstrate our scheme by examining the ionization energy of P-doped Si⟨110⟩ nanowires. We find that there is an effective repulsion between charged P dopants along the nanowire owing to the repulsive interaction of the induced surface charge between adjacent periodic cells. This repulsive interaction decays exponentially with unit cell size instead of a power law behavior assumed in typical charged calculations.

PACS numbers: 73.21.Hb,73.20.Hb

I. INTRODUCTION

Doping is essential in engineering semiconductors with specific electronic properties for various device applications. The dopants in such applications can be neutral, but there are numerous circumstances where charged dopants are of interest. Depending on the experimental conditions, a dopant can be spontaneously ionized. In electronic devices, where the function of dopants is to provide charge carriers, the dopants need to be ionized such that electrons (holes) can be introduced into the conduction (valance) band of the host material. In energy storage devices such as batteries, charged defects are also important. Specifically, the diffusion of charged species are involved during the charging and discharging process of the device. Here we are interested in the behavior of charged defects or dopants at small length scales, *i.e.*, in nanowires. Recently, it is shown that charged impurities play an important role on electron scattering and the electronic transport properties in nanowires[1,2].

We will focus on the formation energy of charged dopants in these systems. This is a key property of charged dopants. However, the formation energy can be a function of the charge state of the dopant and the Fermi level of the system[3] and it can be quite difficult to calculate. *Ab initio* electronic structure calculations of bulk materials commonly impose periodic boundary conditions (supercells) on the domain of the calculation in order to make the calculations tractable. However, the Coulomb interaction between supercells is long-ranged. This results in divergent total energies when a net charge exists in a cell. The divergence is an artifact, which arises solely from imposing periodic boundary conditions in the presence of long range interactions. Real systems are not infinite in extent and such divergences do not exist in experiment. To replicate experimental systems, the long-range Coulomb interactions between supercells should be removed such that the spurious interaction will not occur. This situation led workers to introduce a jellium background into a unit cell for charged calculations. Jellium is a uniform charge distribution, which serves to neutralize the net charge within the unit cell. The jellium screens the long-ranged interactions and results in a finite total energy, even for a system infinite in extent. However, the added jellium need not be passive and the introduction of this charge distribution interacts with the rest of the system. The artificial interaction can be reduced by considering a large supercell as the charge density of the jellium trends to zero as the cell size is increased. Unfortunately, a concurrent increase of the supercell size is deleterious as the computational load of the calculation can increase dramatically with the cell size. An alternative approach proposed by Schultz is to introduce Gaussian charges into the system, instead of a uniform jellium background, to compensate the multipole moments within the unit cell[4,5]. A different approach is the Coulomb-cutoff method which truncates the long-ranged Coulomb interaction along the non-periodic directions[6–8]. For the case of clusters or molecules, the Coulomb interaction can be truncated for all the three directions resulting in a finite total energy[6]. A recent review on this subject can be found in Ref.[9].

A widely used prescription to avoid interactions between the jellium and the system has been proposed by Makov and Payne[10]. In the Makov-Payne scheme, the electrostatic interaction between the periodic array of net charges Z_{net} of the system and the introduced jellium is evaluated using the Madelung sum. The resultant electrostatic energy has the form $\alpha Z_{net}^2/2\epsilon a$, which can be used as a correction to the total energy of the system. Here, a is the

lattice parameter, ϵ is the dielectric constant of the host material, and α is the Madelung constant for the given lattice. Furthermore, Makov and Payne demonstrated that for the case of a molecule with a quadrupole moment, an addition term with $1/a^3$ dependence arises. The screening by the host material is effectively taken into account by the dielectric constant ϵ as a scaling factor[11]. Studies reveal that scaling by ϵ is satisfactory only asymptotically as the cell size increases, or for calculations of molecules well separated by vacuum space, where ϵ is 1[12,13]. Freysoldt *et al.* derived more accurate quantum mechanical corrections for charged dopants within a host material based on first-order perturbation theory[14].

In principle, the study of charged dopants in semiconductor nanowires can be treated similarly as a bulk calculation. The nanowire is placed inside a supercell with sufficient vacuum space in between the periodically repeating array of nanowires. This poses a conceptual problem for charged calculations because the jellium is supposed to fill the nanowires, not the vacuum space in between. Secondly, the Makov-Payne correction should now involve a dielectric tensor instead of a dielectric constant because the charged dopants are separated by the host material only along the axial direction, but are separated by vacuum in the two perpendicular directions[15]. In addition, the corrected total energies still converge slowly with unit cell size[16].

In this paper, we approach the calculation of charged dopants in semiconductor nanowires differently. Instead of using three-dimensional periodic boundary condition as in typical plane wave codes, we adopt only a periodic boundary condition along the wire axis direction. This way, the interaction between different nanowires is removed. We shall show that the divergent interaction between the periodic charged dopants along the wire direction can be removed by appropriately defining the boundary condition for the Kohn-Sham equation *without* introducing a jellium into the calculation. Hence, the resultant total energy is finite and free of the $\sim 1/a$ Madelung error, where a is the periodicity of the nanowire. When compared to plane-wave calculations, our jellium-free scheme does not require Madelung corrections, and avoid the need to calculate the diameter-dependent dielectric tensor of the nanowire. In addition, only a small amount of vacuum space ($\sim$ 5 Å) is necessary in the calculation domain owing to the absence of the artificial inter-wire interaction. Both features offer practical convenience for theoretical studies of charged nanowires. Furthermore, our scheme does not modify or truncate the electrostatic potential as in the Coulomb-cutoff method[6]. We demonstrate our scheme by studying the ionization energy of P-doped Si$\langle 110 \rangle$ nanowires. The convergence rate of ionization energy with respect to the nanowire periodicity is comparable to that of a Madelung-corrected plane-wave calculation. We find that there is induced surface charge after an electron is removed from the P dopant. The induced charge extends far away from P on the nanowire surface. The interaction of induced surface charge between neighboring unit cells is repulsive and exhibits an exponential decay with periodicity a, which is very different from the power law behavior assumed in typical charged calculations.

II. THE ONE-DIMENSIONAL PERIODIC KOHN-SHAM PROBLEM WITH A NET CHARGE

A detailed description of our one-dimensional periodic formalism was presented in previous work[17]. Here, we present a brief review of the formalism, and elaborate only on the parts that are relevant to charged calculations. The electronic structure of a one-dimensional periodic system can be obtained by solving the Kohn-Sham equation[18,19]:

$$\left(\frac{-\hbar^2 \nabla^2}{2m} + V_{ion}[\rho] + V_H[\rho] + V_{xc}[\rho] \right) \psi_{n,k}(\mathbf{r}) = \varepsilon_{n,k} \psi_{n,k}(\mathbf{r}), \tag{1}$$

where V_{ion} is the ion-core pseudopotential, V_H is the Hartree potential, and V_{xc} is the exchange-correlation potential, which is a functional of the ground state electron density ρ. We consider a system periodic in the x direction with a period of a and spatially confined in the y and z directions. A cylindrical domain with radius, L, can be chosen to enclose such system. By Bloch theorem, an eigenstate can be written in the form $\psi_{n,k}(\mathbf{r}) = exp(ikx) u_{n,k}(\mathbf{r})$ where n is the band index and k labels a wave vector in the one-dimensional first Brillouin zone $(-\pi/a, \pi/a)$. $u_{n,k}(\mathbf{r})$ has a periodicity of a along the x direction and vanishes on the boundary of the cylindrical domain. The Kohn-Sham equation can be solved self-consistently after specifying the boundary condition on the cylindrical boundary, which will be explained below.

For the ion-core pseudopotential V_{ion}, we adopt the Kleinman-Bylander form where the pseudopotential is separated into a short-ranged non-local part, and a long-ranged local part[20]. The long-ranged local pseudopotential has an asymptotic behavior of $-Z_i/r$, where Z_i is the ionic charge of an atom i. V_{ion} is evaluated by summing over the atoms within the unit cell and all their periodic images. As explained in Section I, V_{ion} is divergent because the Coulomb interaction is long-ranged. Here, we adopt an Ewald-like technique to evaluate the infinite sum explicitly[21]. For each atom i at position R_i, we add a compensating Gaussian charge $-Z_i$ centered on R_i. Instead of evaluating V_{ion} directly, we evaluate $V_{ion} + V_{com}$, where V_{com} is the electrostatic potential corresponding to the set of compensating Gaussian charges ρ_{com} that we added. Since the long-ranged tail of the local pseudopotential is now canceled by the compensating potential for each atom, the evaluation of $V_{ion} + V_{com}$ involves summing over a finite number of periodic

images. The result is independent of the width of the Gaussian charges. However, an appropriate choice of the width (∼the cut-off radius of the pseudopotential) ensures that $V_{ion}+V_{com}$ converges with only a few periodic images.

V_H is the Hartree potential, which can be solved by the Poisson equation for a given electronic distribution ρ. Since V_{com} is added to V_{ion}, we should solve V_H-V_{com} instead such that the Kohn-Sham equation is not changed. That is, the Poisson equation should be solved for $\rho-\rho_{com}$ within the cylindrical calculation domain of radius L and periodicity a. The boundary condition for the Poisson equation is to specify V_H-V_{com} on the cylindrical surface. Since $\rho-\rho_{com}$ is radially localized within the domain, the boundary condition can be evaluated by a cylindrical multipole expansion[22]. The monopole contribution to the potential on the surface is $V_{0,0}=\frac{2e}{a}Z_{net}\left[\ln 2-\gamma-\ln\frac{L}{a}-(\lim_{2\pi p\to 0}\ln(2\pi p))\right]$, where $Z_{net}=Z_{el}-Z_{ion}$ is the net charge of the system, γ is the Euler constant, e is the charge of an electron, and p is an integer. For one-dimensional periodic charged systems, the divergence is logarithmic. The $\ln\frac{L}{a}$ term can be understood by Gauss's Law for a line charge with charge density $\frac{Z_{net}}{a}$, and the terms corresponding to $\ln 2-\gamma$ represent a boundary condition for Gauss's Law. When the number of electrons Z_{el} equals to the total ionic charge Z_{ion}, Z_{net} is zero, and the monopole will not contribute.

Under our formalism, the specification of the monopole contribution to V_H-V_{com} is crucial for a charged periodic calculation, because this is where the divergence in the Kohn-Sham equation lies. To understand the physics involved, let us consider a one-dimensional periodic array of point charges Z_{net} with periodicity a. We can evaluate the electrostatic potential $V(L)$ at a distance L away and directly on top of one of the point charges. $V(L)$ is calculated by summing up the Coulomb potential $\frac{eZ_{net}}{r}$ from the periodically repeating charges. Asymptotically, $V(L)$ is simply $V_{0,0}$. On the other hand, as $L\to 0$, the near-field formula for $V(L)$ is $\frac{eZ_{net}}{L}-\frac{2e}{a}Z_{net}(\lim_{2\pi p\to 0}\ln(2\pi p))$. This implies that if we are sufficiently close to the system of interest, and drop the logarithmic divergent term, then the electrostatic potential will look as if it corresponds to a non-periodic system. We adopt such a choice for the reference level of V_H-V_{com}, hence the monopole contribution becomes $V_{0,0}=\frac{2e}{a}Z_{net}\left[\ln 2-\gamma-\ln\frac{L}{a}\right]$ without the logarithmic divergence.

There is a corresponding logarithmic divergence in the total energy. The total energy expression is given by:

$$E_{total}=\sum_k\sum_{n=1}^{occ(k)}\varepsilon_n-\frac{1}{2}E_H+\int\rho(\mathbf{r})\left(\varepsilon_{xc}[\rho(\mathbf{r})]-V_{xc}[\rho(\mathbf{r})]\right)d^3\mathbf{r}+E_{ion}, \tag{2}$$

where $E_H=\int V_H(\mathbf{r})\rho(\mathbf{r})\,d^3\mathbf{r}$ is the Hartree energy, E_{ion} is the Coulomb interaction energy between the ions, ε_{xc} is the exchange-correlation energy density which is related to the exchange-correlation potential by $V_{xc}=\delta(\int\rho\varepsilon_{xc}[\rho]\,d^3\mathbf{r})/\delta\rho$. Compared to a neutral calculation, there are two additional terms in the total energy:

$$E_{0,0}=\frac{2\beta e^2}{a}Z_{el}Z_{net}-\frac{e^2Z_{net}^2}{a}(\lim_{2\pi p\to 0}\ln(2\pi p)), \tag{3}$$

where β is $ln2-\gamma-\ln\frac{L}{a}$. The first term corresponds to the electrostatic energy of the total electronic charge Z_{el} under the potential of a line charge with charge density $\frac{Z_{net}}{a}$ given by Gauss's Law. The second term is the logarithmic divergence that should be removed from the total energy, as we did in the Kohn-Sham equation. It corresponds to the electrostatic energy of a periodic array of charges Z_{net} with periodicity a, which is the spurious electrostatic interaction introduced by imposing the periodic boundary condition along the axis direction.

Our formalism for charged one-dimensional periodic calculation is implemented in PARSEC[23,24], which is a real-space code for density functional pseudopotential calculations. We use the local density approximation(LDA). The exchange-correlation functional is from Ceperley and Alder[25] parametrized by Perdew and Zunger[26]. We employ Troullier-Martins pseudopotentials[27] for the ion-core potential V_{ion}. We consider a P-doped Si nanocrystal as a test case for our formalism, and then focus on P-doped Si⟨110⟩ nanowires. ⟨110⟩ nanowires are chosen because it was shown experimentally that they are the most energetically stable configuration for Si nanowires less than ∼ 10 nm in diameter[28]. Our Si nanostructures adopt a bulk-like structure and passivated by H atoms on the surface. One of the Si atoms at the center of the structure is substituted by a P atom. The real space grid is set to be 0.55 a.u., which was shown to be sufficient for the study of ionization energies of P-doped Si nanocrystals[29]. For one-dimensional periodic calculations, only the Γ point is used for the k-point sampling.

III. IONIZATION ENERGY OF A P-DOPED SI NANOCRYSTAL

To test our formalism presented in Section II, we calculate the ionization energy of a small $Si_{34}H_{36}P$ nanocrystal and compare our result to a calculation without imposing any periodic boundary condition (*i.e.* confined boundary condition). The structure of $Si_{34}H_{36}P$ nanocrystal is illustrated in Fig. 1(a). We calculate the ionization energy

IE by $E_i - E_0$, where E_i is the total energy of the ionized P-doped Si nanocrystal with an electron removed, and E_0 is the total energy of the corresponding neutral nanocrystal. Since LDA underestimates the energy gap, there is a corresponding error of the defect level derived from the conduction band minimum for shallow n-type dopants[30]. According to Ref.[31] and[32], the eigenvalue of the defect level from a neutral calculation does not properly take into account the interaction between the defect electron and the induced charge on the nanowire surface owing to LDA self-interaction error. This error propagates to both E_0 and the resultant IE. Hence, the calculation of IE is problematic in addition to the issue of a charged periodic unit cell. In this paper, we focus on the aspect of evaluating the total energy for charged unit cells as described in the previous section, and not the LDA error.

We study the dependence of IE both as a function of L and a. L determines the amount of vacuum space between the nanocrystal surface and the boundary of the cylindrical domain. We find that the total energy E_i is converged when the vacuum space is ~ 5 Å. Hence, we adopt the same amount of vacuum space for all the following calculations. In Fig. 1(b), we illustrate the dependence of IE on periodicity a. $a = 26$ Å corresponds to ~ 10 Å of vacuum space between the periodic images of the nanocrystal. Our result reveals that IE quickly converges to within a few meV with a modest amount of vacuum space between nanocrystals. The eigenvalue spectrum of the ionized $Si_{34}H_{36}P$ nanocrystal is depicted in Fig. 1(c). Apart from small numerical noise, the result from our one-dimensional formalism can reproduce that from the confined boundary condition. Moreover, the eigenvalues are properly referenced with respect to the vacuum.

IV. IONIZATION ENERGY OF P-DOPED SI⟨110⟩ NANOWIRES

In Fig. 2, we illustrate the cross section of our 3 Si⟨110⟩ nanowires with different diameter used in our study. We also show the radial dependence of the self-consistent potentials V_{SCF} for our smallest diameter nanowire (wire 1) in Fig. 2(a). Compared to a neutral nanowire, the V_{SCF} of a charged nanowire with an electron removed is lower in energy. In the vacuum region far away from the nanowire, V_{SCF} of the ionized nanowire exhibits a logarithm behavior as predicted by the Gauss's Law, while the V_{SCF} of the corresponding neutral nanowire decays exponentially.

We examine the dependence of IE on periodicity a by varying a from 27.0 Å to 92.7 Å, which corresponds to repeating the primitive unit cell from 7 to 24 times. Our results are depicted in Fig. 3(a). As a decreases, IE increases, *i.e.*, E_i increases relative to E_0. In the inset of Fig. 3(a), we plot the transition level of wire 1 ($E(0/+) = IE - CBM$) as a function of a, where CBM is the energy of the conduction band minimum of wire 1 without doping. For comparison, the transition level ($E(0/-) = EA - VBM$) of a Al-doped Si⟨110⟩ nanowire with a similar diameter taken from Ref.[16] is also shown. EA is the electron affinity of the Al-doped Si nanowire, and VBM is the energy of the valence band maximum of the wire without doping. Although the dopant in the two studies are different, the inset illustrates that the convergence rate of IE with respect to a for our scheme is comparable to that of a Madelung-corrected plane-wave calculation.

There is an effective repulsion between the ionized P within the nanowire. The log-linear plot in Fig. 3(b) exhibits a linear dependence, which implies that IE as a function of a is exponential, and the repulsive interaction should be quantum mechanical in nature. This behavior is very different from power laws like $1/a$ or $1/a^3$, which are derived from electrostatics and typically used to extrapolate results for charged calculations. Fig. 3(a) shows that the exponential curves fit very well to our calculated results. For our largest diameter nanowire (wire 3), the curve deviates from the exponential fit when the nanowire diameter D is similar or larger than the periodicity a. An exponential decay has also been observed for the P defect wave function in P-doped Si⟨110⟩ nanowires[33].

In order to understand the repulsion between ionized P dopants, we examine the induced charge ρ_{ind} in an ionized P-doped Si⟨110⟩ nanowire. The induced charge ρ_{ind} is obtained by taking the difference between the self-consistent charge density of an ionized P-doped Si⟨110⟩ nanowire (with an electron removed) and the self-consistent charge density of the same but neutral un-doped Si⟨110⟩ nanowire. The total number of electrons are the same for both calculations. Positive (negative) ρ_{ind} indicates electron excess (deficiency) compared to the neutral system. A surface contour plot of ρ_{ind} is drawn in Fig. 4(a) for wire 3. The contour surface corresponds to a positive value of ρ_{ind}. The plot shows that electrons are attracted towards the positively charged P atom. Fig. 4(b) and (c) illustrates the radial dependence of ρ_{ind} for different sections of the P-doped Si⟨110⟩ nanowire. We find that there are electron deficiency on the nanowire surface, *i.e.*, the nanowire surface is positively charged. For sections further away from the charged P atom, ρ_{ind} is smaller in magnitude characterized by negative region near the nanowire surface (the radius of wire 3 is ~ 14 Å). The overall picture is that electrons are drawn from the nanowire surface towards the positively charged P atom, and the induced surface charge extends pretty far away from the P atom. In Fig. 4(d), we compare ρ_{ind} of wire 3 for two different periodicity: $a = 27.0$ Å and $a = 92.7$ Å. For the small periodicity case, ρ_{ind} along the axial direction shrinks to fit inside the unit cell. This demonstrates that the effective repulsion between charged P atoms originates from the repulsion between the induced surface charges from adjacent periodic cells. The behavior of the induced surface charges and their exponentially decaying repulsive interaction should pertain to charged dopants in

both nanowires and nanofilms.

In Fig. 3(c), we examine the dependence of IE on nanowire diameter D. The ionization energies are the extrapolations for $a \to \infty$ from Fig. 3(a), and we denote the asymptotic values by IE_∞. In the same figure, we also indicate the bulk limit obtained by extrapolating the IE of P-doped Si nanocrystals[29]. Note that IE_∞ for nanowires as a function of D does not necessarily trend to the same bulk value obtained from nanocrystals. This is because the ionization energy depends on how the facets of a nanostructure are constructed[34]. Hence, the bulk limit in the figure should be regarded as a guideline. From Fig. 3(c), we find that IE_∞ has a weak dependence on D. By quantum confinement, the eigenvalue of the defect level $-\epsilon_d$ decreases with decreasing diameter as shown in Fig. 3(c). We therefore expect that IE_∞ should decrease significantly with D. However, it is known that the Kohn-Sham eigenvalue obtained from a neutral calculation does not capture the ionization energy, and thus polarization energy stored in a nanomaterial[31,32]. The size-dependent term of this polarization energy is an effective repulsion between the embedded charged P atom and its induced surface charge, which acts against the size-dependence of ϵ_d resulting in a weak size dependence of IE_∞. A similar weak size dependence can also be observed for P-doped Si nanocrystals[29].

V. CONCLUSION

We examined the trend of ionization energy of P-doped Si$\langle 110 \rangle$ nanowire with respect to periodicity and diameter using a one-dimensional periodic formalism in real space. The formalism allows us to remove the spurious interaction of net charges between periodic images, and evaluate the total energy of a charged nanowire. We demonstrate that it is not necessary to introduce a jellium into the calculation cell that interacts with the rest of the system. Without such complications, we find that there is an effective repulsion between charged P atoms which originates from the repulsion between the induced surface charge. The periodicity dependence of the repulsion exhibits an exponential behavior, rather than a power law. Moreover, we find that the ionization energy has a weak diameter dependence resulting from the opposite trend of quantum confinement and polarization effect.

VI. ACKNOWLEDGMENTS

The work was supported in part by the U. S. Department of Energy, Office of Basic Energy Sciences and Office of Advanced Scientific Computing Research from DE-FG02-06ER15760 on nanostructures and DE-SC000187 on algorithms. Work at Rensselaer Polytechnic Institute was supported by the U. S. Department of Energy under Contract No. DE-SC000262. Computational resources were provided in part by the National Energy Research Scientific Computing Center (NERSC), the Texas Advanced Computing Center (TACC), and the Computational Center for Nanotechnology Innovations (CCNI).

[1] R. Rurali, T. Markussen, J. Suñé, M. Brandbyge, and A.-P. Jauho, Nano Lett. **8**, 2825 (2008).
[2] M. P. Persson, H. Mera, Y.-M. Niquet, C. Delerue, and M. Diarra, Phys. Rev. B **82**, 115318 (2010).
[3] S. B. Zhang, and John E. Northrup, Phys. Rev. Lett. **67**, 2339 (1991).
[4] P. A. Schultz, Phys. Rev. B **60**, 1551 (1999).
[5] P. A. Schultz, Phys. Rev. Lett. **84**, 1942 (2000).
[6] M. R. Jarvis, I. D. White, R. W. Godby, and M. C. Payne, Phy. Rev. B **56**, 14972 (1997).
[7] C. A. Rozzi, D. Varsano, A. Marini, E. K. U. Gross, and A. Rubio, Phy. Rev. B **73**, 205119 (2006).
[8] S. Ismail-Beigi, Phy. Rev. B **73**, 233103 (2006).
[9] W. R. L. Lambrecht, physica status solidi (b), doi: 10.1002/pssb.201046327
[10] G. Makov, and M. C. Payne, Phys. Rev. B **51**, 4014 (1995).
[11] M. Leslie, and M. J. Gillan, J. Phys. C **18**, 973 (1985).
[12] A. F. Wright, and N. A. Modine, Phys. Rev. B **74**, 235209 (2006).
[13] C. W. M. Castleton, A. Höglund, and S. Mirbt, Phys. Rev. B **73**, 035215 (2006).
[14] C. Freysoldt, J. Neugebauer, and C. G. Van de Walle, Phys. Rev. Lett. **102**, 016402 (2009).
[15] R. Rurali, and X. Cartoixà, Nano Lett. **9**, 975 (2009).
[16] R. Rurali, M. Palummo, X. Cartoixà, Phys. Rev. B. **81**, 235304 (2010).
[17] J. Han, M. L. Tiago, T.-L. Chan, and J. R. Chelikowsky, J. Chem. Phys. **129**, 144109 (2008).
[18] P. Hohenberg, and W. Kohn, Phys. Rev. **136**, B864 (1964).
[19] W. Kohn, and L. J. Sham, Phys. Rev. **140**, A1133 (1965).
[20] L. Kleinman, and D. M. Bylander, Phys. Rev. Lett. **48** 1425 (1982).
[21] P. P. Ewald, Ann. Phys. **64** 253 (1921).
[22] J. D. Jackson, Classical Electrodynamics, third ed., Wiley, 1998.
[23] J. R. Chelikowsky, J. Phys. D **33**, R33 (2000).
[24] PARSEC has a website at http://parsec.ices.utexas.edu
[25] D. M. Ceperley, and B. J. Alder, Phys. Rev. Lett. **45**, 566 (1980).
[26] J. P. Perdew, and Y. Wang, Phys. Rev. B **45**, 13244 (1992).
[27] N. Troullier, and J. L. Martins, Phys. Rev. B **43**, 1993 (1991).
[28] Y. Wu, Y. Cui, L. Huynh, C. J. Barrelet, D. C. Bell, and C. M. Lieber, Nano Lett. **4**, 433 (2004).
[29] T.-L. Chan, and J. R. Chelikowsky, Nano Lett. **10**, 821-825 (2010).
[30] R. Rurali, B. Aradi, T. Frauenheim, and Á. Gali, Phys. Rev. B. **79**, 115303 (2009).
[31] M. Diarra, Y.-M. Niquet, C. Delerue, and G. Allan, Phys. Rev. B **75**, 045301 (2007).
[32] Y. M. Niquet, L. Genovese, C. Delerue, and T. Deutsch, Phys. Rev. B **81**, 161301(R) (2010).
[33] J. Han, T.-L. Chan, and J. R. Chelikowsky, Phys. Rev. B **82**, 153413 (2010).
[34] C. J. Fall, N. Binggeli, and A. Baldereschi, Phys. Rev. Lett. **88**, 156802 (2002).

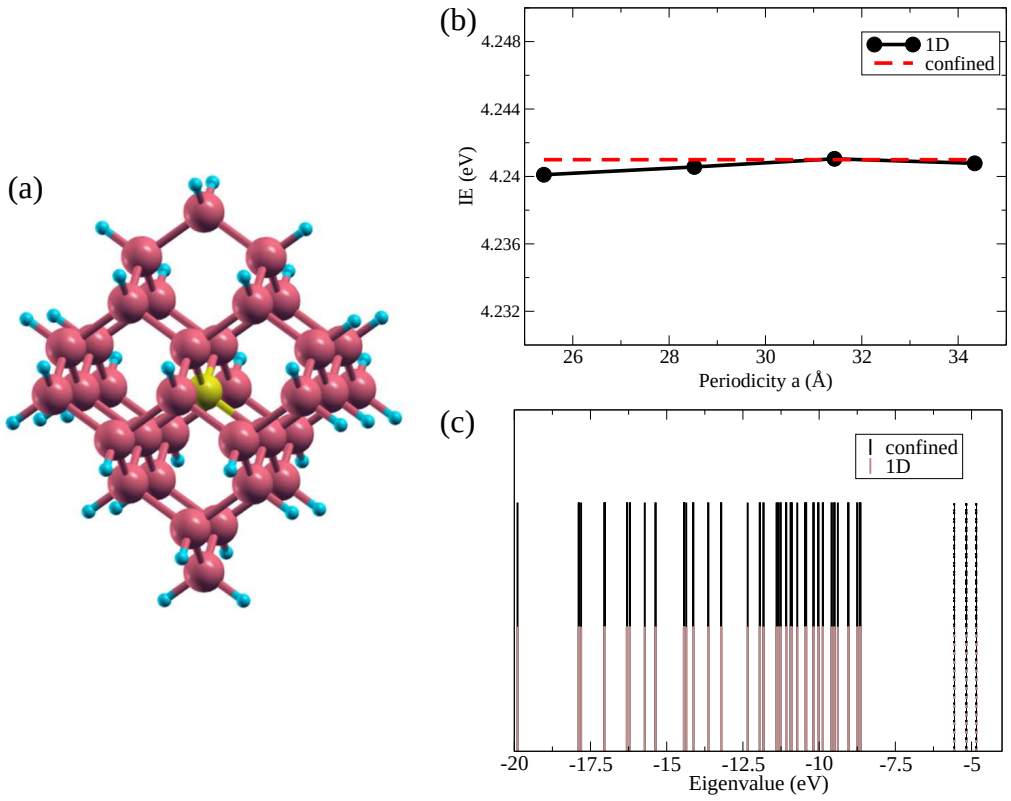

FIG. 1: (a) An atomic model for a $Si_{34}H_{36}P$ nanocrystal. The small spheres on the surface of the nanocrystal are H atoms. The light-shaded atom at the center is P. The rest are Si atoms. (b) Ionization energy (IE) of the $Si_{34}H_{36}P$ nanocrystal plotted as a function of the unit cell periodicity a under one-dimensional periodic boundary condition. The dashed line is obtained by a separate calculation without imposing any periodic boundary condition (confined boundary condition). (c) The eigenvalue spectrum of an ionized $Si_{34}H_{36}P$ nanocrystal with an electron removed. The vertical lines represent the energies of the eigenvalues. Solid lines are for occupied states, and dashed lines are for empty states. Different color corresponds to results using different boundary condition: black for confined boundary condition, gray for one-dimensional periodic boundary condition.

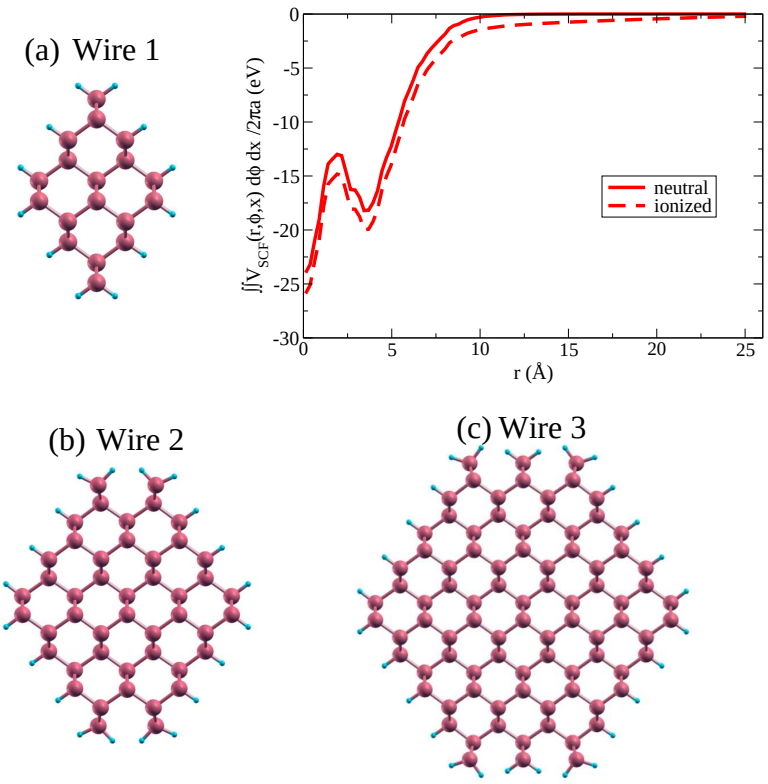

FIG. 2: (a), (b), (c) Atomic models of Si⟨110⟩ nanowires with different diameter. Only the cross section of the nanowires are illustrated. The ⟨110⟩ wire axis points out of the paper. The radial dependence of the self-consistent potentials V_{SCF} for wire 1 are shown (top right). The solid (dashed) line is for a neutral (ionized) wire 1 doped with a P atom at the center.

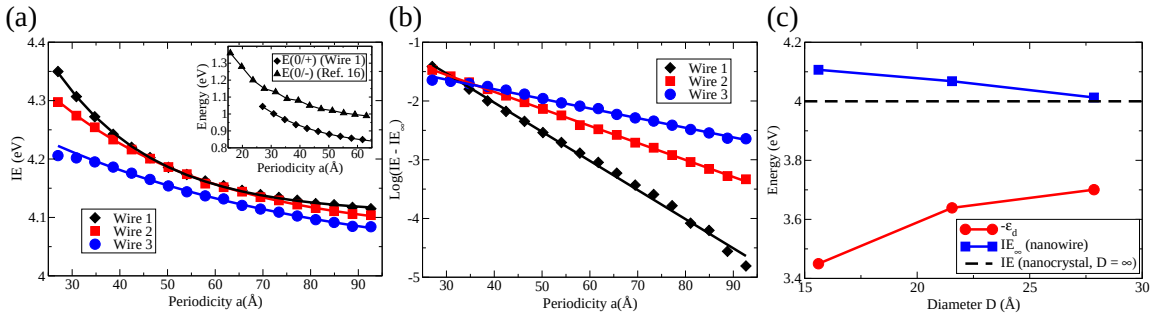

FIG. 3: (a) Ionization energy (IE) of P-doped Si⟨110⟩ nanowires plotted as a function of periodicity a for 3 different wire diameters. The solid lines are fits to the data points using an equation of the form $IE_\infty + Uexp(-a/k)$, where IE_∞, U, and k are fitting parameters. The inset compares the a dependence of the transition level $E(0/+)$ of wire 1 with the transition level $E(0/-)$ of a Al-doped Si⟨110⟩ nanowires from Ref.[16]. (b) A log-linear plot of (a). The asymptotic value IE_∞ is subtracted out from IE first before it is plotted. (c) The diameter D dependence of IE_∞ for P-doped Si⟨110⟩ nanowires (■). The dashed line indicates the bulk limit of IE extrapolated using the data points for P-doped Si nanocrystals[29]. The diameter dependence of the Kohn-Sham eigenvalue of the defect level ($-\epsilon_d$) is also shown (●).

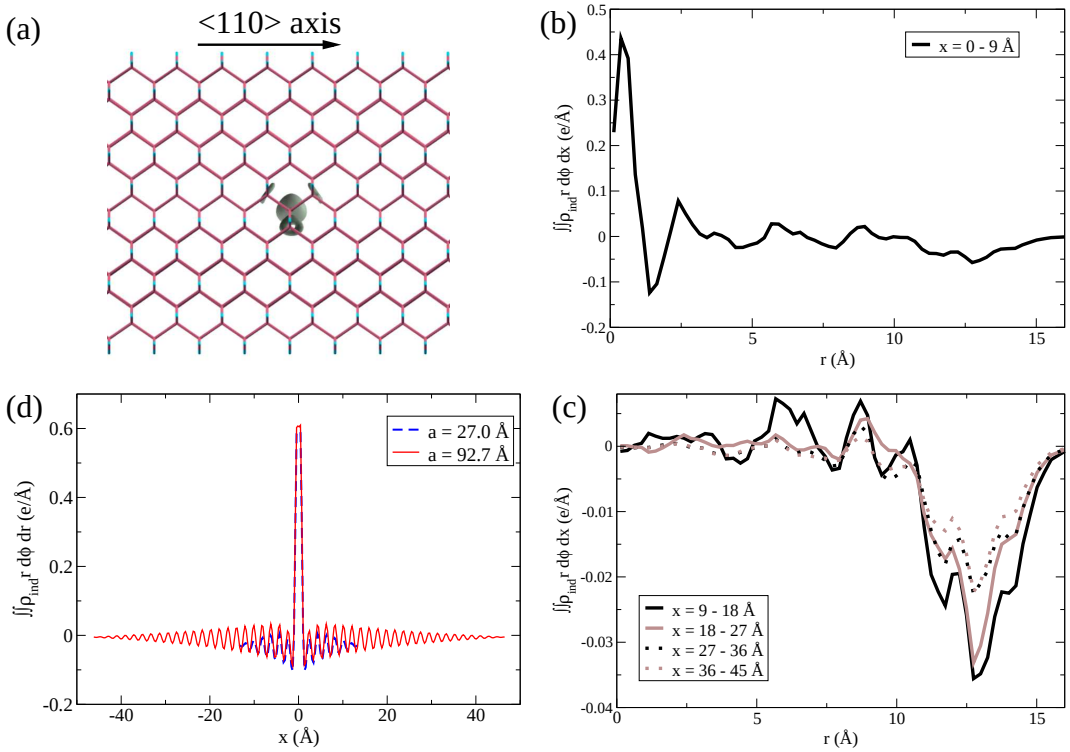

FIG. 4: Induced charge density ρ_{ind} for a P-doped Si⟨110⟩ nanowire (wire 3). Positive (negative) ρ_{ind} indicates an excess (deficiency) of electrons. (a) The side view of a surface contour plot of ρ_{ind} (gray in color). The surface contour corresponds to a positive ρ_{ind} value. Only the atomic bonds are drawn, but not the individual atoms. The P atom is close to the center of the plot, and surrounded by the gray contour surface. (b) and (c) The radial r variation of ρ_{ind} is illustrated for 5 different segments of the nanowire calculated with periodicity $a = 92.7$ Å. The P atom is at $r = 0$ and $x = 0$, where x is the axial coordinate. The segment $x = 0 - 9$ Å contains the charged P atom, while the $x = 36 - 45$ Å segment is furthest away. The radius of the nanowire is ~ 14 Å. (d) The axial variation of ρ_{ind} is depicted for two different periodicity calculated using wire 3.